

A WASp–VASP complex regulates actin polymerization at the plasma membrane

Flavia Castellano, Christophe Le Clainche¹,
Delphine Patin, Marie-France Carlier¹ and
Philippe Chavrier²

Laboratoire de la Dynamique de la Membrane et du Cytosquelette,
Centre National de la Recherche Scientifique UMR 144, Institut Curie,
26 rue d'Ulm, 75241 Paris Cedex 5 and ¹Laboratoire d'Enzymologie
et Biochimie Structurale, CNRS, 91198 Gif-sur-Yvette, France

²Corresponding author
e-mail: Philippe.Chavrier@curie.fr

Proteins of the Wiskott–Aldrich syndrome and Ena/VASP families both play essential functions in the regulation of actin dynamics at the cell leading edge. However, possibilities of functional interplay between members of these two families have not been addressed. Here we show that, in hemopoietic cells, recruitment of the C-terminal VCA (Verprolin homology, Cofilin homology, Acidic) domain of WASp at the plasma membrane by a ligand technique using rapamycin as an intermediate is not sufficient to elicit efficient Arp2/3 complex-mediated actin polymerization. Other domains of WASp, in particular the proline-rich domain, are required for the formation of actin-rich structures. An *in vitro* analysis demonstrates that the proline-rich domain of WASp binds VASP with an affinity of $\sim 10^6$ M⁻¹. In addition, WASp and VASP both accumulate in actin-rich phagocytic cups. Finally, in a reconstituted motility medium, VASP enhances actin-based propulsion of WASp-coated beads in a fashion reminiscent of its effect on *Listeria* movement. We propose that VASP and WASp cooperation is essential in stimulating actin assembly and membrane protrusion at the leading edge.

Keywords: actin/motility/VASP/WASP

Introduction

Actin polymerization is essential for lamellipodial and filopodial protrusion in diverse cellular processes including phagocytosis, cell locomotion, cell polarity and also in intracellular bacterial motility (for review see Borisov and Svitkina, 2000). Nucleation of new actin filaments is spatially controlled by the Arp2/3 complex, a complex of seven evolutionarily conserved proteins (Welch *et al.*, 1997; Machesky and Gould, 1999). Arp2/3 complex activity is stimulated by phosphoinositides and the Rho GTPases Cdc42 and Rac through WASp family proteins that interact with the Arp2/3 complex (Machesky and Insall, 1998; Machesky *et al.*, 1999; Rohatgi *et al.*, 2000). WASp, the product of a hemopoietic specific gene, mutated in the immune-deficiency disorder Wiskott–Aldrich syndrome, and the related more ubiquitous N-WASP protein, bind to and are activated by the

GTP-bound form of Cdc42 and by phosphoinositide 4,5-bisphosphate (PIP₂). Cdc42–GTP interacts with the GTPase-binding domain (GBD) of WASp/N-WASP, while PIP₂ binds a basic region in N-WASP located N-terminally to the GBD domain (Aspenström *et al.*, 1996; Kolluri *et al.*, 1996; Symons *et al.*, 1996; Miki *et al.*, 1998a; Prehoda *et al.*, 2000; Rohatgi *et al.*, 2000). Cdc42–GTP and PIP₂ act synergically to relieve an auto-inhibitory interaction between the C-terminal VCA (Verproline homology, Cofilin homology, Acidic) domain and residues overlapping the GBD (Higgs and Pollard, 2000; Kim *et al.*, 2000; Rohatgi *et al.*, 2000). Once unmasked, VCA binds simultaneously to G-actin and to the Arp2/3 complex, resulting in Arp2/3 complex activation and nucleation of actin filaments (Marchand *et al.*, 2001; for a review see Machesky and Gould, 1999). Altogether, these results indicate that one function of WASp is to regulate actin assembly downstream of Cdc42 and PIP₂ signalling pathways. Moreover, other structural domains of WASp/N-WASP have been shown to interact with various partners involved in the modulation of actin dynamics. The N-terminal EVH1 homology domain binds polyproline sequences in WASp Interacting Protein (WIP), a protein involved in actin reorganization (Ramesh *et al.*, 1997). In addition, a central proline-rich domain (PRD) interacts with profilin and SH3 adaptor proteins, including Grb2 and Nck (Rivero-Lezcano *et al.*, 1995; Miki *et al.*, 1996), which have been shown to enhance N-WASP–Arp2/3 complex-mediated actin assembly (Carlier *et al.*, 2000; Rohatgi *et al.*, 2001). Because of its modular structure, WASp is thus thought to play an essential role in coordinating different signaling routes leading to actin dynamics at the cell leading edge. This assumption is supported by the severe defects in actin-dependent cellular functions including motility, chemotaxis, adhesion and phagocytosis in hemopoietic cells of WAS patients (Zicha *et al.*, 1998; Linder *et al.*, 1999, 2000; Leverrier *et al.*, 2001).

Ena/VASP proteins are members of another protein family implicated in actin dynamics (Gertler *et al.*, 1996). They localize to sites of actin assembly in focal adhesions, to actin-based protrusions at cell–cell contacts, and at the edge of lamellipodia (Reinhard *et al.*, 1992; Rottner *et al.*, 1999; Vasioukhin *et al.*, 2000). VASP is also recruited to the surface of *Listeria monocytogenes* and is required for optimal bacterial motility *in vivo* and *in vitro* (Chakraborty *et al.*, 1995; Niebuhr *et al.*, 1997; Laurent *et al.*, 1999; Loisel *et al.*, 1999). The N-terminal EVH1 domain of VASP targets the protein to specific sites, characterized by F/Y/LPPPP consensus repeats found in the *Listeria* protein ActA (Niebuhr *et al.*, 1997), the focal adhesion proteins zyxin and vinculin (Niebuhr *et al.*, 1997; Drees *et al.*, 2000), Fyb/SLAP protein (Krause *et al.*, 2000) and the guidance factor Robo (Bashaw *et al.*, 2000). However, the

targets of Ena/VASP proteins in lamellipodia and their function in actin dynamics at the leading edge are not precisely known (for review see Machesky, 2000). Some studies (Gertler *et al.*, 1996; Rottner *et al.*, 1999) suggest that Ena/VASP proteins promote actin assembly and cell protrusion at the leading edge. Other recent work indicates that overexpression of VASP results in lowered cell motility while depletion of both VASP and the related protein Mena enhances motility (Bashaw *et al.*, 2000; Bear *et al.*, 2000). Moreover, it is possible that the localization of VASP at the leading edge and at focal adhesions involves different mechanisms (Rottner *et al.*, 1999; Bear *et al.*, 2000; Drees *et al.*, 2000).

The fact that both WASp and VASP control the assembly and organization of actin filaments at the leading edge brought us to investigate the possibility of their coordinated function in actin assembly and motility processes by means of *in vivo* and *in vitro* assay systems. All our data converge to show that VASP cooperates with WASp-Arp2/3 complex to enhance actin-based cellular protrusion.

Results

The C-terminal VCA domain is not sufficient for WASp-mediated actin assembly at the plasma membrane: requirement for the PRD

Various biochemical studies have led to the conclusion that the minimal actin nucleation machinery consists of the Arp2/3 complex interacting with and activated by the conserved C-terminal VCA domain of WASp/Scar proteins, in the presence of G-actin (Higgs *et al.*, 1999; Machesky *et al.*, 1999; Rohatgi *et al.*, 1999; Marchand *et al.*, 2001). It is not known, however, whether this minimal machinery could be sufficient to promote actin assembly at the plasma membrane in living cells. We have addressed this point by targeting the isolated VCA domain of WASp to the plasma membrane using a system that allows for the inducible recruitment of proteins at the cytoplasmic face of the plasma membrane (Castellano *et al.*, 1999). This system, which uses rapamycin as a protein dimerizer *in vivo*, relies on rat basophilic leukemia mast cells (RBL-2H3) that express a chimeric surface receptor. This receptor comprises two copies of a rapamycin-binding FKBP domain as a cytoplasmic region fused with the extracellular/transmembrane region of CD25 (CD25-FKBP₂) (Castellano *et al.*, 1999). CD25-FKBP₂-expressing cells are further transfected with constructs consisting of the FRB domain (a region of the human protein FRAP that binds the FKBP-rapamycin complex) fused with the protein (or portion of the protein) of interest. Upon rapamycin treatment, FRB domain-containing chimeras are induced to associate with the cytoplasmic region of CD25-FKBP₂ with rapamycin acting as a bridge. We recently showed that rapamycin-mediated membrane recruitment of a constitutively activated mutant form of Cdc42 or its downstream effector, WASp, stimulates actin-based membrane protrusion formation (Castellano *et al.*, 1999).

When RBL-2H3 cells expressing the CD25-FKBP₂ receptor and FRB-WASp105-502 (WASp deleted of its first 105 amino acid residues, see Figure 1A for a schematic representation of the constructs used for this

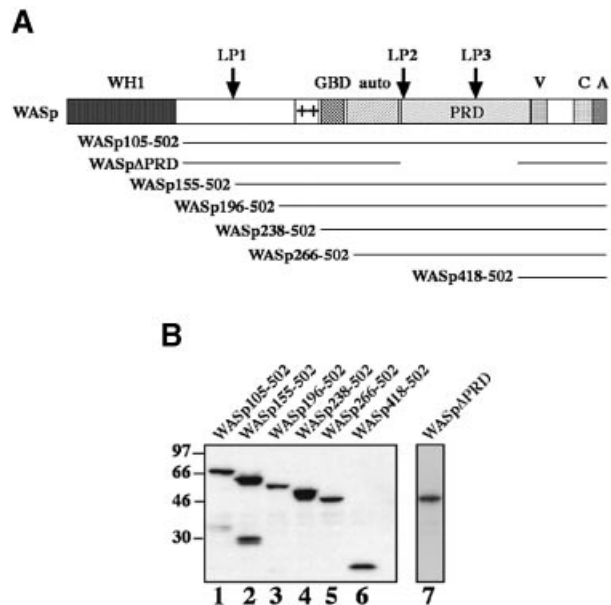


Fig. 1. Schematic representation of the FRB-WASp constructs.

(A) Domain structure of WASp and schematic representation of FRB domain-containing constructs used in this study (the myc tag and the 11 kDa FRB domain fused at the N-terminus of the WASp constructs are not represented). The N-terminus of WASp contains a WH1 domain with similarity to the EVH1 domain of Ena/VASP family proteins. Adjacent to the GBD is a basic region (+), which binds PIP₂ in the case of N-WASp (Rohatgi *et al.*, 2000) and an auto-inhibitory region (auto) that interacts and masks the C-terminal VCA domain. The PRD binds profilin as well as several SH3 domain-containing proteins. The position of three LPPPP motifs (LP1-3) is indicated by arrows. The VCA domain binds actin monomers and the Arp2/3 complex, resulting in stimulation of actin nucleation. (B) Expression levels of FRB chimeras in RBL-2H3 cell lines. Total cell lysates were analyzed by immunoblotting with anti-myc tag antibody.

study) were plated on anti-CD25 antibody-coated glass coverslips to enrich for the receptor at the cell/substratum, and were labeled with fluorescent phalloidin. F-actin was found at the cell periphery and in sparse dots at the ventral surface (Figure 2A). Strikingly, treatment of these cells with rapamycin triggered a strong actin polymerization response localized to the ventral cell surface (Figure 2B). Cells became irregular in shape with numerous actin-rich membrane protrusions. Actin polymerized in the form of short rod-shaped bundles, some of which appeared to connect in a network at the ventral cell surface (Figure 2B, arrows and see inset), and some extending within peripheral protrusions (Figure 2B, arrowheads). Rapamycin-mediated recruitment of activated Cdc42 resulted in a very similar effect (data not shown). A cell line expressing the VCA domain of WASp (position 418-502, see Figure 1A) N-terminally fused to the FRB domain was then examined. Immunoblotting analysis showed that FRB-WASp105-502 and -WASp418-502 were expressed to similar levels in RBL-2H3 cell lines (Figure 1B, compare lanes 1 and 6). In the absence of rapamycin, the distribution of F-actin in these cells did not differ significantly from that in WASp105-502-expressing cells (compare Figure 2C with A); however, in contrast to WASp105-502-expressing cells, treatment of cells expressing WASp418-502 with rapamycin did not result in detectable actin polymerization (Figure 2D). To rule out the possibility that fusion with the

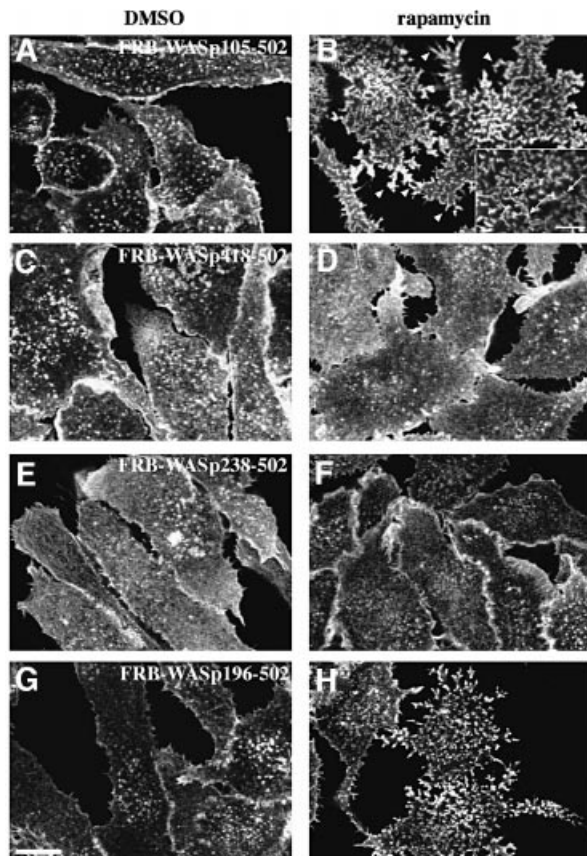


Fig. 2. Requirement for N-terminal regions of WASp in actin assembly. F-actin distribution in stable cell lines expressing the surface receptor CD25–FKBP₂ in combination with various FRB–WASp constructs. Control cells cultured in the absence of rapamycin (A, C, E and G). Membrane translocation of FRB–WASp constructs to the cytoplasmic region of CD25–FKBP₂ receptors was induced by rapamycin treatment (B, D, F and H). Images shown are confocal sections of the ventral cell surface. (A and B) WASp105–502, (C and D) WASp418–502, (E and F) WASp238–502, (G and H) WASp196–502. Bar: 10 μ m.

FRB domain could have impaired the ability of the VCA domain to trigger Arp2/3-mediated actin assembly, FRB–WASp418–502 was transiently overexpressed in BHK-21 cells and compared with the related WA domain of Scar (Machesky and Insall, 1998) for its effect on actin nucleation. When overexpressed to a level 50-fold higher than in the stably transformed RBL-2H3 cell line (see Figure 3A), FRB–WASp418–502 and Scar-WA accumulated as cytoplasmic clusters that were strongly positive for F-actin (Figure 3, compare B–D and E–G), indicating that VCA had retained its capacity to induce actin polymerization when fused with the FRB domain.

A possible explanation for the absence of actin polymerization upon recruitment of the isolated VCA domain to the plasma membrane in RBL-2H3 cells could be that other region(s) of WASp are necessary for stimulating actin assembly at the cell cortex. RBL-2H3 cells expressing CD25–FKBP₂ were therefore transfected with several FRB-tagged constructs extending further toward the N-terminus of WASp (see Figure 1A), and tested for their ability to induce actin polymerization upon rapamycin treatment. Western blotting of cell extracts with anti-myc tag antibodies confirmed that all proteins

migrated at their expected size during SDS–PAGE, and importantly, that they were all expressed to similar levels (Figure 1B). Rapamycin treatment of cells expressing WASp266–502, comprising the PRD and the auto-inhibitory region (Figure 1A; Kim *et al.*, 2000), or WASp238–502, also including the GBD domain, did not induce actin assembly (data not shown and Figure 2E and F, respectively). In contrast, a strong actin polymerization response was induced upon rapamycin treatment of cells expressing WASp196–502 (Figure 2G and H) or WASp155–502 (data not shown), which both include a conserved basic region N-terminal to the GBD domain.

The involvement of the Arp2/3 complex in the rapamycin-induced actin polymerization response was tested by immunofluorescence staining of FRB–WASp418–502- and –WASp105–502-expressing cells with an antibody directed against p41-Arc, a subunit of the Arp2/3 complex (Stewart *et al.*, 1996). In control non-treated cells, the Arp2/3 complex was found in punctate structures that did not coincide with F-actin dots at the ventral surface (Figure 4A, B, E and F). Puncta of Arp2/3 complex were also visible in the entire cell volume (not shown). Rapamycin treatment of cells expressing WASp105–502 triggered a massive accumulation of Arp2/3 complex at the ventral cell surface where it colocalized with F-actin-rich structures (Figure 4G and H). Therefore, actin polymerization in response to WASp recruitment correlated with an accumulation of Arp2/3 complex in actin-rich structures. In contrast, the distribution of Arp2/3 complex remained unchanged upon rapamycin treatment of cells expressing WASp418–502 (Figure 4C and D).

Altogether, these data demonstrated that the VCA domain was not sufficient to activate actin assembly at the plasma membrane, and pointed at a critical role of the central part of WASp comprising regions flanking and including the GBD domain, as well as the PRD. Contribution of the PRD region of WASp in actin assembly was assessed by expressing a truncated form of WASp carrying a deletion of the entire PRD (WASp Δ PRD, see Figure 1A). As shown in Figure 5, rapamycin treatment of WASp Δ PRD-expressing cells did not induce actin polymerization, demonstrating the essential role of the PRD region in WASp-mediated actin assembly.

The PRD of WASp interacts with VASP

Examination of the amino acid sequence of the central region of WASp revealed the presence of three LPPPP motifs at position 159–163 (LP1), 313–319 (LP2) and 381–387 (LP3). The Ena/VASP homology 1 (EVH1) domain of Ena/VASP family members involved in the regulation of actin dynamics binds to proteins containing proline-rich sequences with a consensus motif F/W/Y/LPPPP (Niebuhr *et al.*, 1997). In addition, a sequence in the cytoplasmic domain of the *Drosophila* receptor Robo with a core LPPPP motif has recently been shown to mediate a direct interaction with Ena (Bashaw *et al.*, 2000). Therefore, we have tested the possibility that the WASp PRD region could be involved in an interaction with VASP.

Pulldown assays first showed that glutathione *S*-transferase (GST) fusion proteins of WASp comprising the PRD region immobilized on glutathione–Sepharose were

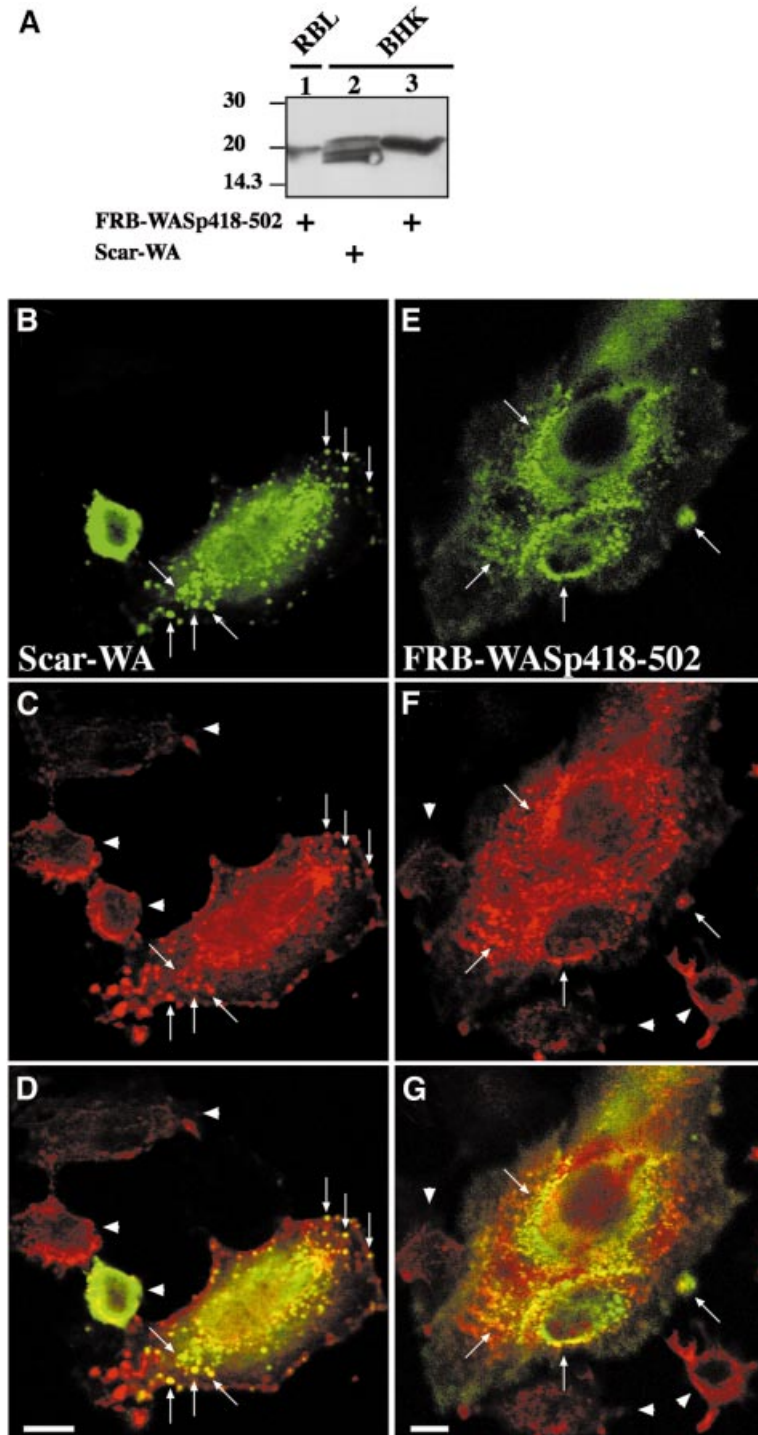


Fig. 3. Overexpressed FRB-WASp418-502 induces F-actin clusters in BHK-21 cells. (A) Lysates of RBL-2H3 cell line expressing FRB-WASp418-502, or BHK-21 cells overexpressing FRB-WASp418-502 or Scar-WA were run on 12% SDS-PAGE (9 μ g total protein per lane) and blotted on to PVDF. Blots were revealed using mouse anti-myc tag antibody (clone 9E10) and the ECL procedure. The signal in RBL-2H3 cells is ~5-fold less than in BHK-21 cells (compare lanes 1 and 3). Taking into consideration that ~10% of BHK-21 cells expressed the FRB-WASp418-502 protein, we estimate that the level of expression of FRB-WASp418-502 is ~50-fold lower in the RBL-2H3 stable cell line compared with that in BHK-21 cells. (B-D) BHK-21 cells expressing the Scar-WA domain. (E-G) BHK-21 cells expressing the FRB-WASp418-502 construct. (B and E) Localization of myc-tagged constructs as revealed using anti-myc tag antibody. (C and F) Distribution of F-actin. Arrows point at clusters of WASp or Scar C-terminal domains and F-actin. Arrowheads show non-transfected cells. (D and G) Superimposition of anti-myc and F-actin images. Bar: 10 μ m.

able to bind VASP present in RBL-2H3 cells (Figure 6A, WASp155-502 and 155-429, lanes 5-6). In contrast, VASP did not interact with a construct lacking residues 310-418 corresponding to the PRD (WASp Δ PRD, lane 8),

nor did it bind to the isolated VCA domain or GST control (lanes 7 and 4, respectively). Binding of VASP was not modified when extracts of RBL-2H3 cells activated by cross-linking of the IgE receptor (Fc ϵ RI) were used

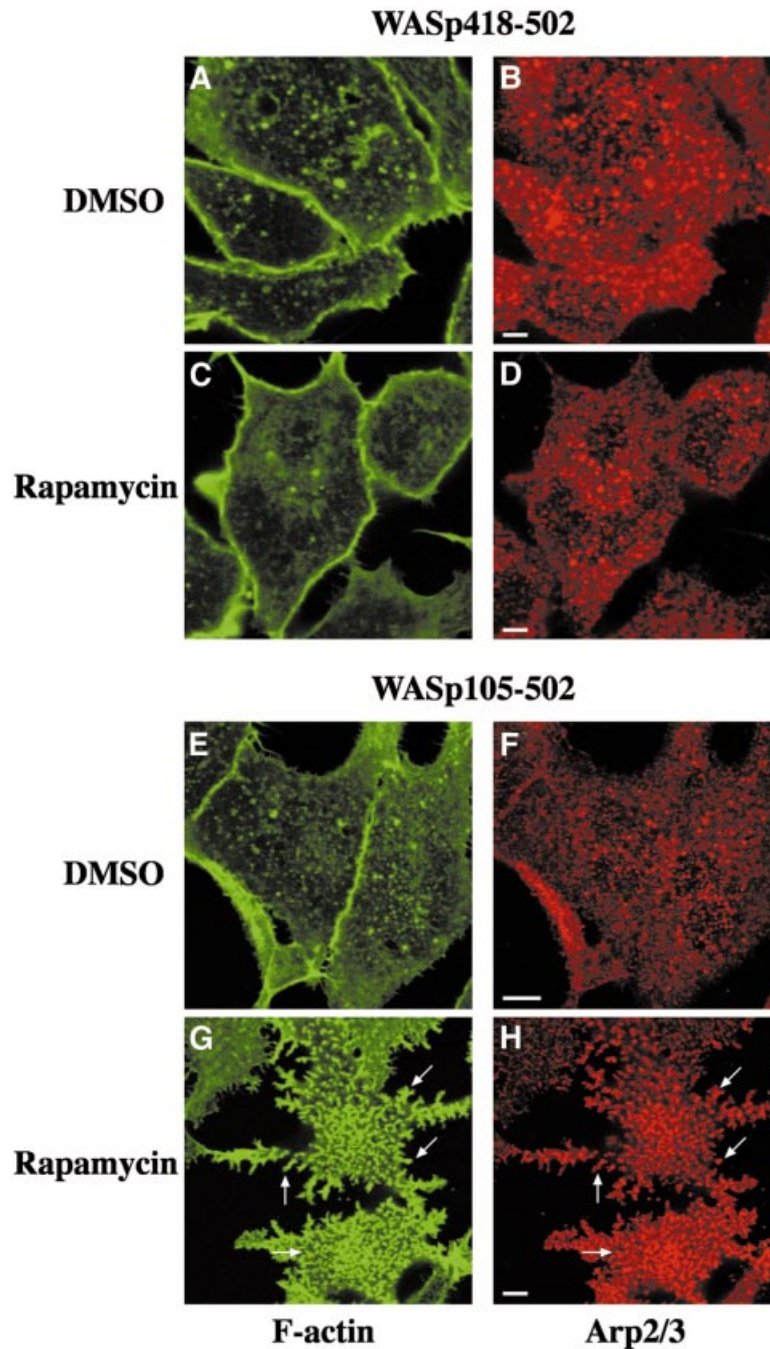


Fig. 4. Immunofluorescence localization of the Arp2/3 complex in cell lines expressing the isolated VCA domain (WASp418–502) or WASp105–502. RBL-2H3 cell lines expressing FRB–WASp418–502 (A–D) or FRB–WASp105–502 (E–H) were plated on to glass coverslips coated with anti-CD25 antibodies and treated with DMSO as control (A, B, E and F) or rapamycin (C, D, G and H), fixed, and stained with phalloidin (A, C, E and G) and anti-p41Arc, a subunit of the Arp2/3 complex (B, D, F and H). Confocal sections were recorded at the level of the ventral surface. Bar: 5 μ m.

(lanes 9–13), indicating that interaction of VASP with WASp does not require cell activation. Binding of VASP to immobilized WASp was also observed when lysates of non-hemopoietic Baby Hamster Kidney (BHK-21) cells were used (data not shown).

To examine whether WASp and VASP interact directly, purified polyhistidine-tagged VASP (Laurent *et al.*, 1999) was incubated with the various GST–WASp constructs bound to glutathione–Sepharose beads. Figure 6B shows that recombinant His₆–VASP bound to GST–WASp155–

502 and WASp155–429 (lane 12–13), but did not interact with the construct lacking the PRD region (WASp Δ PRD, lane 10), nor to the VCA domain (lane 11). These results, confirming the pull-down experiments, indicate that VASP interacts directly with WASp, and that this interaction requires an intact PRD region. A GST construct comprising residues 155–390 of WASp was sufficient for the interaction with recombinant VASP, further confirming the implication of most of the PRD region to the interaction with VASP (Figure 6C, lanes 3–8, Bound).

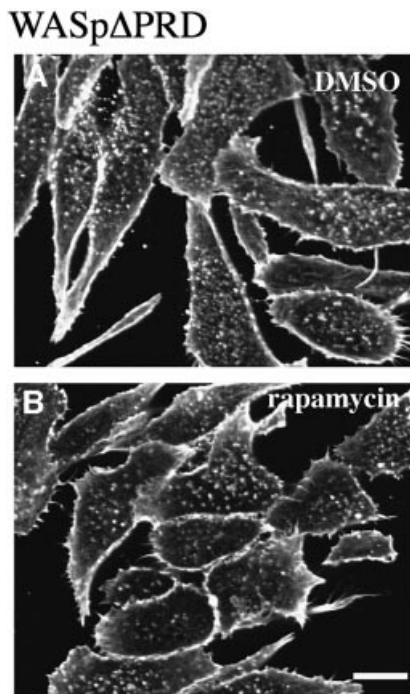


Fig. 5. Deletion of the PRD region of WASp abolishes actin assembly. F-actin distribution in RBL-2H3 cells expressing FRB–WASp Δ PRD with a deletion of the PRD (position 155–390, see Figure 1A). (A) Control cells in the absence of rapamycin. (B) Cells treated with rapamycin. Confocal sections were recorded at the level of the ventral surface. Bar: 10 μ m.

This construct was used to estimate the affinity of the WASp–VASP complex. Purified recombinant VASP (50 nM) was incubated in the presence of increasing concentrations of WASp155–390 and a fixed amount of glutathione–Sepharose beads, and uncomplexed VASP remaining in the supernatant was quantified by immunoblotting analysis (Figure 6C, lanes 3–8, Unbound). The binding of WASp155–390 to VASP reached 90% saturation at a concentration of WASp of 6 μ M, and half-maximal binding was observed at 1 μ M WASp. From these data we evaluated the equilibrium dissociation constant for binding of VASP to WASp155–390 at \sim 1 μ M (see Materials and methods).

Presence of VASP in WASp-mediated actin-rich structures

The distribution of VASP was investigated in FRB–WASP105–502-expressing cells. In the absence of rapamycin, VASP was clearly enriched in F-actin-rich membrane ruffles at the cell periphery (Figure 7A and B, arrows), and in structures located inside the cells at the level of the ventral surface (arrowheads). Rapamycin addition triggered a dramatic redistribution of VASP in F-actin bundles that formed as a consequence of membrane recruitment of FRB–WASP105–502 (Figure 7C and D, arrowheads depict internal structures labelled for F-actin and VASP, while arrows point at protrusions). In contrast, the distribution of VASP was not affected upon rapamycin treatment of FRB–WASP418–502-expressing cells (data not shown). Therefore, rapamycin-mediated

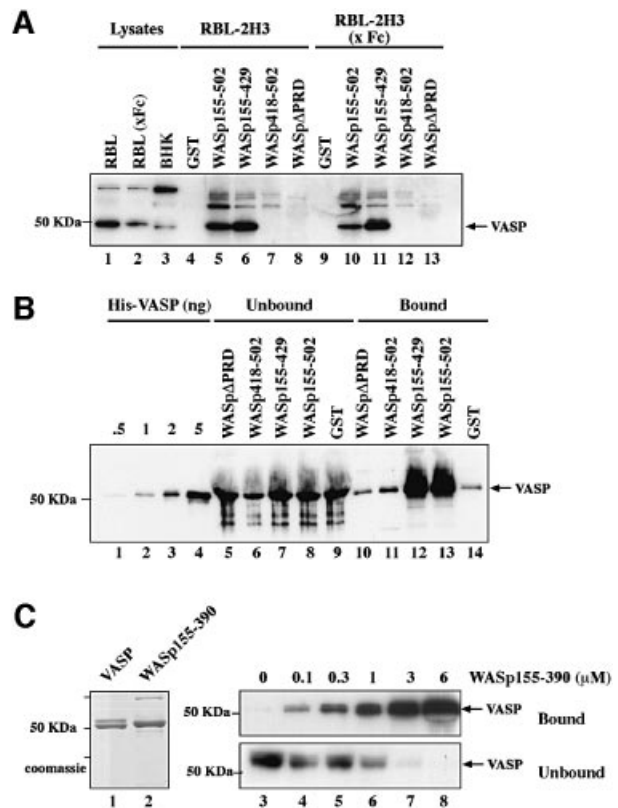


Fig. 6. The PRD of WASp mediates direct interaction with VASP. (A) VASP pull-down from RBL-2H3 cell lysates using the GST–WASP fusion proteins indicated. GST, GST–WASP155–502, –WASP155–429, –WASP418–502 (VCA domain) or –WASP Δ PRD (WASP155–502 deleted of the PRD, position 310–390) immobilized on glutathione–Sepharose beads was incubated with cell lysates prepared from unstimulated RBL-2H3 cells, or cells stimulated by cross-linking of Fc ϵ RI (x Fc). Bound material was subjected to western blotting with anti-VASP antibodies. Lanes 1–3: total cell lysates; lanes 4–8: GST pull-down from RBL-2H3 cell lysate; lanes 9–13: GST pull-down from lysate of RBL-2H3 cells activated by Fc ϵ RI cross-linking. (B) The central PRD of WASp mediates direct binding to VASP. GST or GST–WASP fusion proteins (1 μ g) bound to glutathione–Sepharose beads were incubated with recombinant His₆–VASP (250 nM) and bound material was subjected to western blotting with anti-VASP antibodies. Lanes 1–4: the indicated amount of His₆–VASP; lanes 5–9: unbound material (2% of total); lanes 10–14: bound material (50% of total). (C) Estimation of the equilibrium binding constant of VASP with WASp155–390. His₆–VASP or GST–WASP(155–390)His₆ (1 μ g each) was visualized by Coomassie Blue staining of the gel (lanes 1 and 2). VASP (50 nM) was incubated in the presence of increasing concentrations of WASp155–390 as indicated, in the presence of a fixed amount of glutathione–Sepharose beads. Bound and unbound proteins were subjected to SDS–PAGE followed by western blotting with anti-VASP antibody (lanes 3–8). A value of \sim 1 μ M was derived for the equilibrium binding constant for VASP with WASp155–390. The results shown are representative of four independent experiments with two different preparations of recombinant proteins.

recruitment of WASp to CD25–FKBP₂ receptors induces the accumulation of VASP at sites of actin assembly.

Then, the presence of WASp and VASP was assessed during phagocytosis, a physiological process requiring actin filament assembly (Chimini and Chavrier, 2000). Phagocytosis of antibody-coated particles bound to Fc receptors is regulated by Cdc42 and Rac and involves the Arp2/3 complex (Caron and Hall, 1998; Massol *et al.*, 1998; May *et al.*, 2000). Overexpressed WASp/N–WASP, as well as the p34–Arc subunit of the Arp2/3 complex

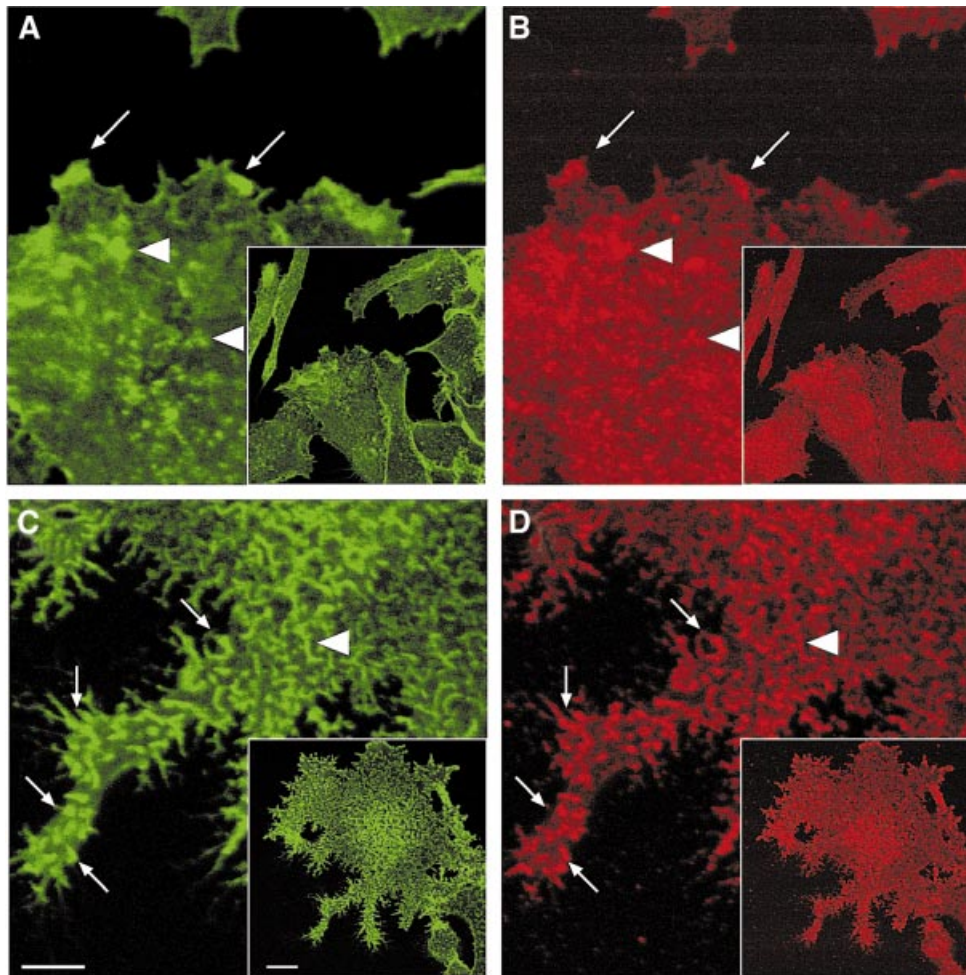


Fig. 7. Immunofluorescence localization of VASP in WASp105–502-expressing cell line. RBL-2H3 cells expressing FRB–WASp105–502 were plated on to glass coverslips coated with anti-CD25 antibodies and treated with DMSO as control (A and B) or rapamycin (C and D), fixed, and stained with phalloidin (A and C) and anti-VASP antibodies (B and D). Lower magnification fields are shown in the insets. Arrows point at peripheral structures positive for F-actin and VASP, while arrowheads depict internal structures. Confocal sectioning was performed at the ventral cell surface. Bar: 10 μm .

co-localize with F-actin in phagocytic cups (Lorenzi *et al.*, 2000; May *et al.*, 2000). As we previously reported (Massol *et al.*, 1998), incubation of RBL-2H3 cells in the presence of IgE-coated particles triggered the formation of actin-rich phagocytic cups surrounding the particles (Figure 8A and B). Immunofluorescence staining demonstrated that endogenous WASp (Figure 8C and D) and VASP (Figure 8E and F) were both enriched in phagocytic cups.

Actin-based motility of WASp-coated beads is enhanced by VASP

To examine whether the complex of WASp and VASP affects cellular protrusion, we analyzed the effect of VASP on the propulsion of WASp-coated beads in a minimal motility medium reconstituted from pure proteins (Loisel *et al.*, 1999). In this medium, the ActA–Arp2/3 complex-induced movement of *Listeria* was strongly enhanced by VASP (Loisel *et al.*, 1999). On the other hand, WASp-coated microspheres have been demonstrated to undergo actin-based propulsion in cell extracts (Yarar *et al.*, 1999). To obtain WASp-coated beads, extracts of transfected

BHK-21 cells overexpressing myc-tagged FRB–WASp155–502 were first treated with poly-L-proline–Sepharose to deplete endogenous VASP, then incubated with 2.8 μm diameter Dynabeads coated with anti-myc antibodies. Successful removal of VASP from the extracts, and adsorption of WASp on the beads was confirmed by immunoblotting (data not shown and Figure 9A). The WASp-coated beads were placed in the motility medium, in the absence or presence of VASP. Short, irregular, dense comet tails were seen in the absence of VASP (Figure 9C–F), but the rate of movement was lower than 0.1 $\mu\text{m}/\text{min}$ (Table I). Addition of VASP (0.5 μM) enhanced the rate of movement to 0.93 $\mu\text{m}/\text{min}$ (Table I). Increased motility correlated with an 8-fold increase in the length of actin tails (Table I and Figure 9G–I). Addition of a 1.6 μM GST fusion of the proline-rich region of ActA (ActA^{Pro241–323}), which binds to the EVH1 domain of VASP, induced a 3-fold decrease in the rate of movement and length of the actin tails (Table I and Figure 9J–M). These data establish that the interaction of VASP, probably mediated by the EVH1 domain, with the PRD of WASp stimulates actin-based

RBL-2H3 (FcR-mediated phagocytosis)

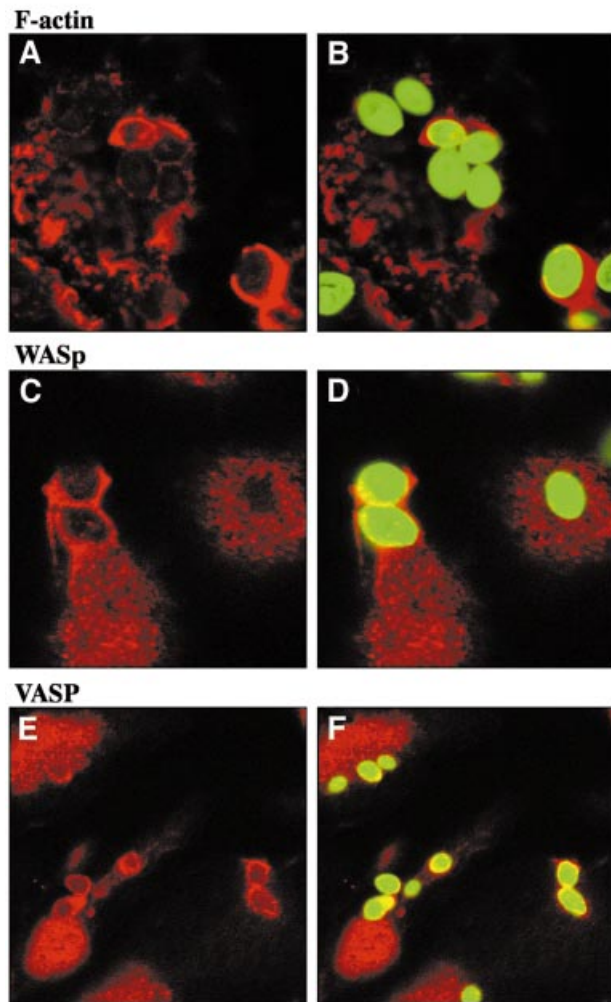


Fig. 8. Accumulation of WASp and VASP in actin-rich phagocytic cups during FcR-mediated phagocytosis. RBL-2H3 cells that express the high affinity IgE receptor (FcεRI) were incubated with IgE-opsonized zymosan particles. After 30 min at 37°C, cells were fixed and labeled with Texas Red–phalloidin to visualize F-actin (A and B), with anti-WASp antibodies (C and D) or antibodies specific for VASP (E and F). Zymosan particles, visualized in the FITC channel, are shown in green in (B), (D) and (F). Confocal optical sections were recorded in the dorsal plane of the cells. Bar, 10 µm.

motility *in vitro* as well as actin assembly at the plasma membrane *in vivo*.

Discussion

The present work provides new insights into the mechanism of regulation of WASp as well as the function of VASP in actin-based membrane protrusion and motility processes. We first show that although the C-terminal VCA domain of WASp triggers the formation of cytoplasmic F-actin clusters when overexpressed to a high level *in vivo*, in agreement with its effect on Arp2/3-induced actin polymerization *in vitro*, WASp-mediated actin assembly at the plasma membrane requires, in addition to the VCA, domains spanning the basic region,

the GBD and the proline-rich region. The latter turned out to be essential. Secondly, we demonstrate that VASP interacts directly with WASp both *in vivo* and *in vitro* with an estimated binding constant of $\sim 1 \mu\text{M}$, and that this interaction is mediated by the WASp PRD region. The association of VASP with WASp accounts for the observed localization of the two proteins in WASp-induced actin-based structures in the rapamycin assay and for their accumulation in the phagocytic cup. Thirdly, VASP binding to WASp immobilized on beads greatly enhances actin-based propulsion of the beads in a minimal motility medium, an effect reminiscent of the enhancement of *Listeria* movement by VASP.

The recent dissection of the WASp/N-WASP structure–function relationship (Higgs and Pollard, 2000; Kim *et al.*, 2000; Prehoda *et al.*, 2000; Rohatgi *et al.*, 2000) has shown that the transition from a ‘closed’ auto-inhibited to an ‘open’ active conformation requires several domains of WASp/N-WASP including the basic region, the GBD and the VCA domain. Furthermore, cooperative binding of PIP₂ and Cdc42 to the basic region and to the GBD, respectively, activates WASp/N-WASP. Our results provide evidence for the significance of the regulatory process in a membrane-linked context *in vivo*. WASp constructs starting at position 266 and 238 contain the auto-inhibitory region C-terminally adjacent to the GBD and are defective in the rapamycin system. In contrast, WASp chimeras starting at a more N-terminal position (105, 155 or 196) are competent for promoting actin assembly upon rapamycin-induced targeting to the plasma membrane. These constructs comprise a basic region N-terminal to the GBD (position 225–235, including five lysine residues), which is conserved in the related N-WASP protein where it mediates PIP₂ binding (Rohatgi *et al.*, 2000). It is reasonable to assume that the basic region of WASp may similarly bind PIP₂. Therefore, our data strongly support the view that in a cellular context, in the actual membrane environment, exposure to PIP₂ leads to the activation of WASp by relieving the auto-inhibition.

Paradoxically, clustering of VCA at the plasma membrane fails to stimulate actin assembly and protrusion. This result suggests that in this targeting system, VCA, although being constitutively active, may not be positioned in a productive fashion. In addition, the PRD of WASp appears to be critical since its deletion abolishes WASp-mediated actin assembly in the rapamycin system. This domain is known to bind SH3 domain effectors of WASp such as Grb2 or Nck, which cooperate with PIP₂ (Carlier *et al.*, 2000; Rohatgi *et al.*, 2001) and Cdc42 (Carlier *et al.*, 2000) to recruit and activate WASp (i.e. relieve the ‘closed’ auto-inhibited conformation), and in turn to promote Arp2/3-mediated actin assembly. Here, we document a direct interaction between the WASp PRD region, which contains LPPPP motifs, and VASP with a binding constant of $\sim 1 \mu\text{M}$. This interaction is 20- to 60-fold stronger than that of the VASPEVH1 domain with peptides derived from either the third tandem repeat of *Listeria* ActA or the fourth FPPPP repeat of zyxin (Ball *et al.*, 2000). The value of $1 \mu\text{M}$ found for the K_d indicates that the WASp–VASP complex must form in relevant amounts in hemopoietic cells, since physiological concentrations of $10 \mu\text{M}$ VASP (in neutrophils; Higgs and Pollard, 2000) and $4 \mu\text{M}$ VASP (in platelets; Laurent *et al.*,

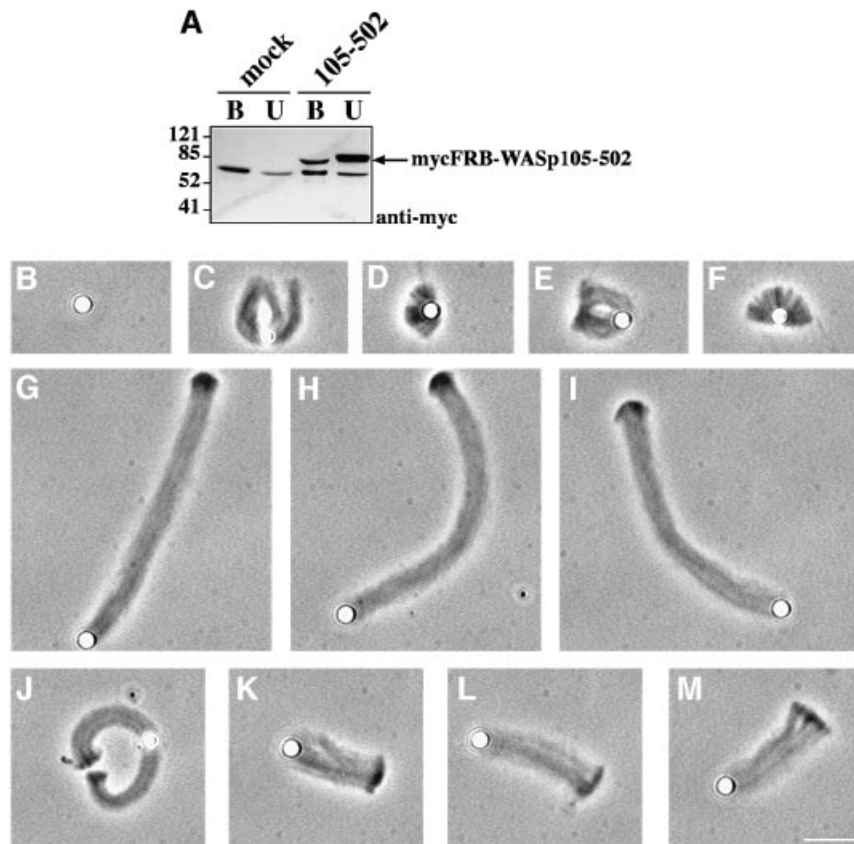


Fig. 9. Effect of VASP on reconstituted actin-based motility of WASp-coated beads. (A) Extract of BHK-21 cells overexpressing mycFRB-WASp105-502 or control mock-transfected cell extract were incubated with anti-myc tag antibody-coated beads. Unbound proteins (U) or proteins bound to anti-myc beads (B) were subjected to western blot analysis with anti-myc tag antibody. (B-M) Typical phase-contrast images of beads after 90 min of incubation in the reconstituted motility medium. (B) Control bead. (C-F) MycFRB-WASp105-502-coated beads in the motility medium in the absence of VASP. (G-I) Motility medium supplemented with 0.5 μ M VASP or (J-M) supplemented with 0.5 μ M VASP and 1.6 μ M GST-ActAPro241-323. Bar, 10 μ m.

Table I. Rate of movement of WASp105-502-coated beads in the reconstituted motility assay

	Maximal rate of movement (μ m/min)	Tail length at $t = 90$ min (μ m)
WASp105-502	<0.1	4.43 \pm 1.78 ($n = 4$)
WASp105-502 + VASP	0.93 \pm 0.11 ($n = 10$)	36.88 \pm 6.11 ($n = 10$)
WASp105-502 + VASP + GST-ActAPro241-323	0.35 \pm 0.08 ($n = 11$)	12.13 \pm 1.76 ($n = 8$)

1999) have been reported. In addition, the hemopoietic protein Fyb/SLAP has been shown recently to associate with Ena/VASP family proteins (through a FPPPPDDDI sequence), and to be part of a complex including also WASp, Nck and SLP-76 (Krause *et al.*, 2000). Together with these data, the evidence in the present study indicates that the interactions linking WASp- and VASP-mediated pathways in modulating actin assembly could be both direct and indirect. Remarkably, LPPPP motifs are absent from the PRD of N-WASp. Moreover, we have found that N-WASp is unable to compete the binding of WASp to VASP (data not shown). These findings suggest that N-WASp and VASP function independently, an assumption supported by the observation that N-WASp-mediated actin-based movement of *Shigella* does not require VASP (Egile *et al.*, 1999). In contrast, L/IPPPP motifs are found in the related proteins Scar/WAVE-1 and -2 (Miki *et al.*,

1998b; Suetsugu *et al.*, 1999). WAVE-1 and the Ena/VASP family protein, Mena, colocalize at the lamellipodium edge (Nakagawa *et al.*, 2001). In addition, Scar/WAVE proteins interact with and recruit the Abelson tyrosine kinase (c-Abl) to lamellipodia (Westphal *et al.*, 2000), while protein partners of Abl (Abis) colocalize with VASP to sites of actin assembly at the tips of lamellipodia and filopodia (Stradal *et al.*, 2001). Therefore, our findings concerning the role of VASP in WASp function may apply to Scar/WAVE proteins, and suggest a potential mechanism for targeting VASP at the cell leading edge.

Actin-based motility assays of WASp-coated beads in a biochemically defined medium leave no doubt about the positive effect of VASP on actin-based motility. The effect of VASP on the propulsion of WASp-coated beads is remarkably similar to its effect on actin-based movement of *Listeria* (Chakraborty *et al.*, 1995; Smith *et al.*, 1996;

Niebuhr *et al.*, 1997; Laurent *et al.*, 1999; Loisel *et al.*, 1999) or ActA-coated beads (Boujemaa *et al.*, 2001). In both cases, the effect of VASP is mediated by interaction of the EVH1 domain with a PRD adjacent to an Arp2/3 activating domain, suggesting a common mechanism. The effect of VASP on WASp- or ActA-associated motility processes contrasts with the absence of effect of VASP on Cdc42-induced actin assembly in neutrophil extracts, which is also mediated by WASp (Yang *et al.*, 2000). Notably, in the aforementioned study the amount of assembled F-actin was quantified, but the actin-based movement of particles or foci on which actin was assembled was not monitored. Similarly, *in vitro*, VASP does not affect the process of actin assembly and filament branching induced by ActA-Arp2/3, while it enhances the movement of ActA-coated beads (Boujemaa *et al.*, 2001). Hence VASP may act in a manner different from other regulators of WASp such as PIP₂, Cdc42, the *Shigella* protein IcsA or Grb-2.

Our results support a coordinated role for WASp and VASP in actin-based cell protrusion specific to hemopoietic cells. A role for VASP in actin dynamics at the lamellipodia was first suggested by Rottner and colleagues who observed a correlation between the amount of VASP at the leading edge and the rate of lamellipodium extension in motile cells (Rottner *et al.*, 1999). Similarly, overexpressed Mena, an Ena/VASP family member, triggers the formation of actin-rich protuberances in fibroblasts (Gertler *et al.*, 1996). In addition, WASp, the Arp2/3 complex and VASP are present in protruding regions of the plasma membrane in hemopoietic cells in actin-rich phagocytic cups and at contact sites of T lymphocytes with their targets (Chimini and Chavrier, 2000; Krause *et al.*, 2000; Lorenzi *et al.*, 2000; May *et al.*, 2000; this study). On the other hand, our results are difficult to reconcile with recent work, indicating that overexpression of VASP slows down cells while depletion of both VASP and Mena enhances motility (Bashaw *et al.*, 2000; Bear *et al.*, 2000). These contradictory findings may be due to the different experimental systems used, and/or the different cellular functions of VASP in motility and adhesion. Elucidation of this puzzle will require further experimentation.

Materials and methods

FRB chimera construction and stable transfection in RBL-2H3 cells

CD25-FKBP₂, Cdc42V12-FRB and FRB-WASp105-502 have been described previously (Castellano *et al.*, 1999). The mycFRB domain fused constructs: FRB-WASp155-502, -WASp196-502, -WASp238-502, -WASp266-502, -WASp418-502 and -WASpΔPRD (fragment 105-310 in-frame with fragment 418-502) were obtained by PCR using PWO polymerase (Roche). The PCR products were cloned into pGEM1-mycFRB (Castellano *et al.*, 1999) and verified by sequencing. The different FRB-containing chimeras were subcloned in the mammalian expression vector pS α -Puro and stably transfected into the RBL-2H3-derived cell line (15B), expressing the chimeric membrane protein CD25-FKBP₂ (Castellano *et al.*, 1999). Cells were selected with puromycin (Sigma-Aldrich Co.) as described (Castellano *et al.*, 1999).

Transient transfection in BHK-21 cells

BHK-21 cells were transfected with Eugene 6 (Roche) according to the manufacturer's instructions. Cells were fixed 40 h post-transfection and processed for immunofluorescence labelling with 9E10 anti-myc tag monoclonal antibody to recognize epitope-tagged FRB-WASp418-502 and Scar-WA (Machesky and Insall, 1998) constructs and with Texas

Red-conjugated phalloidin (Molecular Probes, Eugene, OR) to label actin structures.

Confocal immunofluorescence microscopy

For Texas Red-labelled phalloidin and anti-VASP (rabbit polyclonal M4 antibody, ImmunoGlobe GmbH, Grossostheim, Germany) staining, cells were fixed in 3% paraformaldehyde followed by permeabilization in 0.1% Triton X-100 for 4 min. For Arp2/3 complex labeling with anti-p41 Arc antibody (a kind gift from Dr H.Higgs), cells were permeabilized for 2 min in 3.5% formaldehyde, 5% sucrose, 0.1% Triton X-100 and then fixed for 1 h in the same buffer without Triton X-100. For WASp labelling (Ab 3D8.H5; Stewart *et al.*, 1996), cells were fixed in 3.7% formaldehyde followed by permeabilization in acetone. Fluorescent secondary antibodies were obtained from Jackson Immunoresearch. Optical sections were taken with Leica TCS 4D and TCS SP2 confocal microscopes.

GST fusion proteins and purification

Different domains of human WASp: WASp155-502, -418-502 (VCA), -155-429, -ΔPRD (fragment 105-310 in-frame with fragment 418-502) have been expressed as GST fusion proteins by inserting the corresponding DNA fragments from pSR α -Puro in a modified version of pGEX-4T-1 with an extra *SpeI* site. GST-WASp(155-390)His₆ was obtained by a PCR-based approach by addition of a His₆ tag in the 3'-end oligonucleotide and insertion in pGEX-4T-1. All constructs were verified by sequencing. Plasmids were introduced into the bacterial strain BL21-(DE3) by transformation and protein expression was induced by the addition of 0.5 mM isopropyl- β -D-thiogalactopyranoside (IPTG). Bacteria were lysed in 50 mM Tris-HCl pH 7.5, 1 mM DTT, 0.5 mM EDTA, 150 mM NaCl, 0.2 mg/ml hen egg lysozyme, 5 mM MgCl₂, 3 unit/ml DNase I and protease inhibitors (Complete Protease Inhibitor Cocktail, Roche). After clearing the bacterial lysate by centrifugation at 10 000 g for 15 min, GST fusion proteins were bound to glutathione-Sepharose beads (Amersham Pharmacia Biotech) following the manufacturer's instructions. Purified proteins were analyzed by SDS-PAGE and quantified by comparison with bovine serum albumin (BSA) as standard. WASp155-390 was expressed as a fusion protein with both a C-terminal polyhistidine tag, and an N-terminal GST tag. After IPTG induction as above, the bacterial lysate was submitted to a first step of purification on Ni-NTA-agarose (Qiagen). After extensive washing of the resin, bound material was eluted in phosphate-buffered saline (PBS) supplemented with 0.2 M imidazole. The protein in the eluate was subsequently purified by binding to glutathione-Sepharose beads as described above. This two-step/two-tag procedure ensured purification of full-length WASp155-390 without contamination by truncated products. Production and purification of polyhistidine-tagged VASP from baculovirus-infected insect cells has been described previously (Laurent *et al.*, 1999).

GST pulldown assay

GST pulldown were performed by incubating 5 μ g GST fusion proteins bound to glutathione-Sepharose beads (50 μ l bed volume) in the presence of 200 μ g of total proteins from RBL-2H3 cell lysate in lysis buffer (10 mM Tris-HCl pH 7.5, 150 mM NaCl, 1% NP-40, 1 mM NaVO₄, 10 mM NaF supplemented with protease inhibitors). When indicated, RBL-2H3 cells were activated by 15 min cross-linking of Fc ϵ R1 with 1 μ g/ml anti-rat Fc ϵ R1 α chain (clone BC4, a gift from Dr R.P.Siraganian, NIH, Bethesda, MD). Incubations were performed with rotation at 4°C for 2 h. Beads were washed in lysis buffer and bound proteins were eluted by boiling the beads in SDS sample buffer. Proteins were separated by 10% SDS-PAGE and blotted on to polyvinylidene fluoride (PVDF). Blots were stained using rabbit M4 anti-VASP antibodies and the ECL procedure (Amersham Pharmacia Biotech).

VASP-WASp interaction

Direct binding of WASp to VASP was assessed by incubating 1 μ g GST-WASp constructs bound to glutathione-Sepharose beads (10 μ l) with 250 nM purified His₆-VASP in K buffer (50 mM Tris-HCl pH 7.5, 200 mM NaCl, 1 mM EDTA) supplemented with 0.5% Triton X-100 and 1% BSA (KTB buffer) for 2 h. After three washes in K buffer, bound material was analyzed by western blotting using anti-VASP M4 antibodies. Determination of the affinity of the WASp-VASP complex was measured by incubating 50 nM His₆-VASP in KTB buffer in the presence of increasing concentrations of GST-WASp155-390 (0, 0.1, 0.3, 1, 3 and 6 μ M) bound to glutathione-Sepharose beads (bead bed volume was kept constant at 10 μ l). Unbound His₆-VASP in supernatants was quantified by immunoblotting with anti-VASP M4 antibodies,

followed by ECF procedure (Amersham Pharmacia Biotech). K_d was calculated according to the formula: $K_d = [\text{VASP}]_{\text{free}} \times [\text{WASPpPRD}]_{\text{free}} / [\text{WASP:VASP}]$, taking the value of 45 kDa for the molecular mass of VASP (i.e. monomeric form).

Anti-CD25 antibody coating experiments

Glass coverslips 12 mm in diameter in 24-well plates were coated with 2.5 μg of anti-human CD25 mouse monoclonal antibody (clone B1.49.9, Immunotech, Marseille, France) in 250 μl of PBS for 4 h at 37°C. After washing in PBS, 2×10^5 cells were seeded per well. After 2 h, cells were treated overnight with 100 nM rapamycin (Sigma-Aldrich Co.) in dimethylsulfoxide (DMSO) or the equivalent volume of DMSO for control.

Assay for Fc ϵ R1-mediated phagocytosis

RBL-2H3 cells grown on glass coverslips were incubated for 30 min at 37°C in the presence of fluoresceinated DNP-conjugated zymozan particles coated with rat anti-DNP IgE (clone LO-DNP30, LO-IMEX, Brussels, Belgium) as described previously (Massol *et al.*, 1998). Cells were then fixed and processed for analysis by confocal immunofluorescence microscopy.

In vitro actin-based motility assay

Preparation of WASp-coated beads. Total proteins were extracted from mock transfected BHK-21 cells as a control or from BHK-21 cells overexpressing mycFRB-WASP105-502 in 50 mM Tris-HCl pH 7.5, 150 mM NaCl, 1 mM EDTA, 1% NP-40, 0.25% sodium deoxycholate, 1 mM phenylmethylsulfonyl fluoride supplemented with Complete protease inhibitors. Extracts were incubated twice with poly-L-proline (Sigma-Aldrich) bound to CNBr-activated Sepharose 4B (Amersham Pharmacia Biotech) in order to deplete endogenous VASP. Goat anti-mouse IgG-coated magnetic dynabeads (100 μl of 1% 2.8 μm diameter beads, Dynal) were incubated with 20 μg of 9E10 anti-myc antibody and 20 μg of irrelevant mouse IgG in XB buffer (10 mM HEPES pH 7.5, 100 mM KCl, 1 mM MgCl₂, 0.1 mM CaCl₂, 0.5% BSA) for 1 h at 4°C on a rotating wheel and washed twice with XB buffer. Beads were then incubated with 250 μl of mycFRB-WASP105-502 containing extract or control extract for 1 h at 4°C on a rotating wheel and washed twice with XB buffer.

Motility assay. Actin-based motility of WASp-coated beads was reconstituted *in vitro* as in Loisel *et al.* (1999). The motility medium consisted of 10 mM Tris-HCl pH 7.5, 1.5 mM Mg-ATP, 5 mM DTT, 100 mM KCl, 6.5 μM F-actin, 0.1 μM Arp2/3, 0.05 μM capping protein, 4 μM actin-depolymerizing factor (ADF), 2 μM profilin, 0.2 μM α -actinin, 0.3% methylcellulose, 4 mg/ml BSA and 4×10^6 /ml mycFRB-WASP105-502-coated beads or control beads were added to this medium. When indicated, medium was supplemented with 0.5 μM His₆-tagged VASP (Laurent *et al.*, 1999) and 1.3 μM ActA241-323 (corresponding to the proline-rich VASP-binding domain of ActA) as indicated. Samples were prepared for phase contrast optical microscopy as described previously (Egile *et al.*, 1999; Laurent *et al.*, 1999) and rates of movement were determined by measuring the bead displacement over a period of 4 min.

Acknowledgements

We are indebted to Drs Aepfelbacher, E.Friedrich, H.N.Higgs, L.M.Machesky, D.L.Nelson, R.P.Siraganian and J.Weiland for the gift of valuable reagents. We also thank Dr J.Plastino and W.Hempel for critical reading of the manuscript, and D.Meur for expert photographic work. F.C. was a recipient of a fellowship from the Institut Curie. This work was supported by CNRS institutional funding and grants from the Institut Curie, the Fondation pour la Recherche Médicale (INE20000407009/1), the Association pour la Recherche sur le Cancer (ARC 5449) to P.C. and the Ligue Nationale contre le Cancer to M.-F.C.

References

Aspenström, P., Lindberg, U. and Hall, A. (1996) Two GTPases, CDC42 and Rac, bind directly to a protein implicated in the immunodeficiency disorder Wiskott-Aldrich syndrome. *Curr. Biol.*, **6**, 70-75.
 Ball, L.J. *et al.* (2000) Dual epitope recognition by the VASP EVH1 domain modulates polyproline ligand specificity and binding affinity. *EMBO J.*, **19**, 4903-4914.
 Bashaw, G.J., Kidd, T., Murray, D., Pawson, T. and Goodman, C.S. (2000)

Repulsive axon guidance: Abelson and Enabled play opposing roles downstream of the roundabout receptor. *Cell*, **101**, 703-715.
 Bear, J.E., Loureiro, J.J., Libova, I., Fassler, R., Weiland, J. and Gertler, F.B. (2000) Negative regulation of fibroblast motility by Ena/VASP proteins. *Cell*, **101**, 717-728.
 Borisy, G.G. and Svitkina, T.M. (2000) Actin machinery: pushing the envelope. *Curr. Opin. Cell Biol.*, **12**, 104-112.
 Boujemaa-Paterski, R. *et al.* (2001) *Listeria* protein ActA mimics WASP family proteins: it activates filament barbed end branching by Arp2/3 complex. *Biochemistry*, **40**, in press.
 Carlier, M.F. *et al.* (2000) GRB2 links signaling to actin assembly by enhancing interaction of neural Wiskott-Aldrich syndrome protein (N-WASP) with actin-related protein (ARP2/3) complex. *J. Biol. Chem.*, **275**, 21946-21952.
 Caron, E. and Hall, A. (1998) Identification of two distinct mechanisms of phagocytosis controlled by different Rho GTPases. *Science*, **282**, 1717-1721.
 Castellano, F., Montcourrier, P., Guillemot, J.C., Gouin, E., Machesky, L.M., Cossart, P. and Chavrier, P. (1999) Inducible recruitment of Cdc42 or WASP to a cell-surface receptor triggers actin polymerization and filopodium formation. *Curr. Biol.*, **9**, 351-360.
 Chakraborty, T. *et al.* (1995) A focal adhesion factor directly linking intracellularly motile *Listeria monocytogenes* and *Listeria ivanovii* to the actin-based cytoskeleton of mammalian cells. *EMBO J.*, **14**, 1314-1321.
 Chimini, G. and Chavrier, P. (2000) Function of rho family proteins in actin dynamics during phagocytosis and engulfment. *Nature Cell Biol.*, **2**, E191-E196.
 Drees, B., Friederich, E., Fradelizi, J., Louvard, D., Beckerle, M.C. and Golsteyn, R.M. (2000) Characterization of the interaction between zyxin and members of the Ena/vasodilator-stimulated phosphoprotein family of proteins. *J. Biol. Chem.*, **275**, 22503-22511.
 Egile, C., Loisel, T.P., Laurent, V., Li, R., Pantaloni, D., Sansonetti, P.J. and Carlier, M.F. (1999) Activation of the CDC42 effector N-WASP by the *Shigella flexneri* IcsA protein promotes actin nucleation by Arp2/3 complex and bacterial actin-based motility. *J. Cell Biol.*, **146**, 1319-1332.
 Gertler, F.B., Niebuhr, K., Reinhard, M., Weiland, J. and Soriano, P. (1996) Mena, a relative of VASP and *Drosophila* Enabled, is implicated in the control of microfilament dynamics. *Cell*, **87**, 227-239.
 Higgs, H.N. and Pollard, T.D. (2000) Activation by Cdc42 and PIP₂ of Wiskott-Aldrich syndrome protein (WASP) stimulates actin nucleation by Arp2/3 complex. *J. Cell Biol.*, **150**, 1311-1320.
 Higgs, H.N., Blanchoin, L. and Pollard, T.D. (1999) Influence of the C terminus of Wiskott-Aldrich syndrome protein (WASP) and the Arp2/3 complex on actin polymerization. *Biochemistry*, **38**, 15212-15222.
 Kim, A.S., Kakalis, L.T., Abdul-Manan, N., Liu, G.A. and Rosen, M.K. (2000) Autoinhibition and activation mechanisms of the Wiskott-Aldrich syndrome protein. *Nature*, **404**, 151-158.
 Kolluri, R., Tolia, K.F., Carpenter, C.L., Rosen, F.S. and Kirshhausen, T. (1996) Direct interaction of the Wiskott-Aldrich syndrome protein with the GTPase Cdc42. *Proc. Natl Acad. Sci. USA*, **93**, 5615-5618.
 Krause, M., Sechi, A.S., Konradt, M., Monner, D., Gertler, F.B. and Weiland, J. (2000) Fyn-binding protein (Fyb)/SLP-76-associated protein (SLAP), Ena/vasodilator-stimulated phosphoprotein (VASP) proteins and the Arp2/3 complex link T cell receptor (TCR) signaling to the actin cytoskeleton. *J. Cell Biol.*, **149**, 181-194.
 Laurent, V., Loisel, T.P., Harbeck, B., Wehman, A., Gröbe, L., Jockusch, B.M., Weiland, J., Gertler, F.B. and Carlier, M.F. (1999) Role of proteins of the Ena/VASP family in actin-based motility of *Listeria monocytogenes*. *J. Cell Biol.*, **144**, 1245-1258.
 Leverrier, Y., Lorenzi, R., Blundell, M.P., Brickell, P., Kinnon, C., Ridley, A.J. and Thrasher, A.J. (2001) The Wiskott-Aldrich syndrome protein is required for efficient phagocytosis of apoptotic cells. *J. Immunol.*, **166**, 4831-4834.
 Linder, S., Nelson, D., Weiss, M. and Aepfelbacher, M. (1999) Wiskott-Aldrich syndrome protein regulates dosomes in primary human macrophages. *Proc. Natl Acad. Sci. USA*, **96**, 9648-9653.
 Linder, S., Higgs, H., Hufner, K., Schwarz, K., Pannicke, U. and Aepfelbacher, M. (2000) The polarization defect of Wiskott-Aldrich syndrome macrophages is linked to dislocalization of the Arp2/3 complex. *J. Immunol.*, **165**, 221-225.
 Loisel, T.P., Boujemaa, R., Pantaloni, D. and Carlier, M.F. (1999) Reconstitution of actin-based motility of *Listeria* and *Shigella* using pure proteins. *Nature*, **401**, 613-616.
 Lorenzi, R., Brickell, P.M., Katz, D.R., Kinnon, C. and Thrasher, A.J.

- (2000) Wiskott–Aldrich syndrome protein is necessary for efficient IgG-mediated phagocytosis. *Blood*, **95**, 2943–2946.
- Machesky,L.M. (2000) Putting on the brakes: a negative regulatory function for Ena/VASP proteins in cell migration. *Cell*, **101**, 685–688.
- Machesky,L.M. and Gould,K.L. (1999) The Arp2/3 complex: a multifunctional actin organizer. *Curr. Opin. Cell Biol.*, **11**, 117–121.
- Machesky,L.M. and Insall,R.H. (1998) Scar1 and the related Wiskott–Aldrich syndrome protein, WASP, regulate the actin cytoskeleton through the Arp2/3 complex. *Curr. Biol.*, **8**, 1347–1356.
- Machesky,L.M., Mullins,R.D., Higgs,H.N., Kaiser,D.A., Blanchoin,L., May,R.C., Hall,M.E. and Pollard,T.D. (1999) Scar, a WASP-related protein, activates nucleation of actin filaments by the Arp2/3 complex. *Proc. Natl Acad. Sci. USA*, **96**, 3739–3744.
- Marchand,J.B., Kaiser,D.A., Pollard,T.D. and Higgs,H.N. (2001) Interaction of WASP/Scar proteins with actin and vertebrate Arp2/3 complex. *Nature Cell Biol.*, **3**, 76–82.
- Massol,P., Montcourrier,P., Guillemot,J.C. and Chavrier,P. (1998) Fc receptor-mediated phagocytosis requires CDC42 and Rac1. *EMBO J.*, **17**, 6219–6229.
- May,R.C., Caron,E., Hall,A. and Machesky,L.M. (2000) Involvement of the Arp2/3 complex in phagocytosis mediated by FcγR or CR3. *Nature Cell Biol.*, **2**, 246–248.
- Miki,H., Miura,K. and Takenawa,T. (1996) N-WASP, a novel actin-depolymerizing protein, regulates the cortical cytoskeletal rearrangement in a PIP2-dependent manner downstream of tyrosine kinases. *EMBO J.*, **15**, 5326–5335.
- Miki,H., Sasaki,T., Takai,Y. and Takenawa,T. (1998a) Induction of filopodium formation by a WASP-related actin-depolymerizing protein N-WASP. *Nature*, **391**, 93–96.
- Miki,H., Suetsugu,S. and Takenawa,T. (1998b) WAVE, a novel WASP-family protein involved in actin reorganization induced by Rac. *EMBO J.*, **17**, 6932–6941.
- Nakagawa,H., Miki,H., Ito,M., Ohashi,K., Takenawa,T. and Miyamoto,S. (2001) N-WASP, WAVE and Mena play different roles in the organization of actin cytoskeleton in lamellipodia. *J. Cell Sci.*, **114**, 1555–1565.
- Niebuhr,K. *et al.* (1997) A novel proline-rich motif present in ActA of *Listeria monocytogenes* and cytoskeletal proteins is the ligand for the EVH1 domain, a protein module present in the Ena/VASP family. *EMBO J.*, **16**, 5433–5444.
- Prehoda,K.E., Scott,J.A., Dyrche Mullins,R. and Lim,W.A. (2000) Integration of multiple signals through cooperative regulation of the N-WASP–Arp2/3 complex. *Science*, **290**, 801–806.
- Ramesh,N., Anton,I.M., Hartwig,J.H. and Geha,R.S. (1997) WIP, a protein associated with Wiskott–Aldrich syndrome protein, induces actin polymerization and redistribution in lymphoid cells. *Proc. Natl Acad. Sci. USA*, **94**, 14671–14676.
- Reinhard,M., Halbrugge,M., Scheer,U., Wiegand,C., Jockusch,B.M. and Walter,U. (1992) The 46/50 kDa phosphoprotein VASP purified from human platelets is a novel protein associated with actin filaments and focal contacts. *EMBO J.*, **11**, 2063–2070.
- Rivero-Lezcano,O.M., Marcilla,A., Sameshima,J.H. and Robbins,K.C. (1995) Wiskott–Aldrich syndrome protein physically associates with Nck through Src homology 3 domains. *Mol. Cell Biol.*, **15**, 5725–5731.
- Rohatgi,R., Ma,L., Miki,H., Lopez,M., Kirchhausen,T., Takenawa,T. and Kirschner,M.W. (1999) The interaction between N-WASP and the Arp2/3 complex links Cdc42-dependent signals to actin assembly. *Cell*, **97**, 221–231.
- Rohatgi,R., Ho,H.Y. and Kirschner,M.W. (2000) Mechanism of N-WASP activation by CDC42 and phosphatidylinositol 4,5-bisphosphate. *J. Cell Biol.*, **150**, 1299–1310.
- Rohatgi,R., Nollau,P., Ho,H.Y., Kirschner,M.W. and Mayer,B.J. (2001) Nck and phosphatidylinositol 4,5-bisphosphate synergistically activate actin polymerization through the N-WASP–Arp2/3 pathway. *J. Biol. Chem.*, **276**, 26448–26452.
- Rottner,K., Hall,A. and Small,J.V. (1999) Interplay between Rac and Rho in the control of substrate contact dynamics. *Curr. Biol.*, **9**, 640–648.
- Smith,G.A., Theriot,J.A. and Portnoy,D.A. (1996) The tandem repeat domain in the *Listeria monocytogenes* ActA protein controls the rate of actin-based motility, the percentage of moving bacteria, and the localization of vasodilator-stimulated phosphoprotein and profilin. *J. Cell Biol.*, **135**, 647–660.
- Stewart,D.M., Treiber-Held,S., Kurman,C.C., Facchetti,F., Notarangelo,L.D. and Nelson,D.L. (1996) Studies of the expression of the Wiskott–Aldrich syndrome protein. *J. Clin. Invest.*, **97**, 2627–2634.
- Stradal,T., Courtney,K.V., Rottner,K., Hahne,P., Small,J.V. and Pendergast,A.M. (2001) The Abl interactor proteins localize to sites of actin polymerization at the tips of lamellipodia and filopodia. *Curr. Biol.*, **11**, 891–895.
- Suetsugu,S., Miki,H. and Takenawa,T. (1999) Identification of two human WAVE/SCAR homologues as general actin regulatory molecules which associate with the Arp2/3 complex. *Biochem. Biophys. Res. Commun.*, **260**, 296–302.
- Symons,M., Derry,J.M.J., Kariak,B., Jiang,S., Lemahieu,V., McCormick,F. and Abo,A. (1996) Wiskott–Aldrich syndrome protein, a novel effector for the GTPase CDC42Hs, is implicated in actin polymerization. *Cell*, **84**, 723–734.
- Vasioukhin,V., Bauer,C., Yin,M. and Fuchs,E. (2000) Directed actin polymerization is the driving force for epithelial cell–cell adhesion. *Cell*, **100**, 209–219.
- Welch,M.D., Iwamatsu,A. and Mitchison,T.J. (1997) Actin polymerization is induced by Arp2/3 protein complex at the surface of *Listeria monocytogenes*. *Nature*, **385**, 265–269.
- Westphal,R.S., Soderling,S.H., Alto,N.M., Langeberg,L.K. and Scott,J.D. (2000) Scar/WAVE-1, a Wiskott–Aldrich syndrome protein, assembles an actin-associated multi-kinase scaffold. *EMBO J.*, **19**, 4589–4600.
- Yang,C., Huang,M., DeBiasio,J., Pring,M., Joyce,M., Miki,H., Takenawa,T. and Zigmond,S.H. (2000) Profilin enhances Cdc42-induced nucleation of actin polymerization. *J. Cell Biol.*, **150**, 1001–1012.
- Yarar,D., To,W., Abo,A. and Welch,M.D. (1999) The Wiskott–Aldrich syndrome protein directs actin-based motility by stimulating actin nucleation with the Arp2/3 complex. *Curr. Biol.*, **9**, 555–558.
- Zicha,D., Allen,W.E., Brickell,P.M., Kinnon,C., Dunn,G.A., Jones,G.E. and Thrasher,A.J. (1998) Chemotaxis of macrophages is abolished in the Wiskott–Aldrich syndrome. *Br. J. Haematol.*, **101**, 659–665.

Received July 25, 2001; revised August 28, 2001;
accepted August 29, 2001